

# 산업단지의 지표온도 조사 및 IR 카메라를 이용한 플랜트구조물의 비파괴평가

Tran Quang Huy · 허정원<sup>†</sup> · Nguyen Truong Linh · 한동엽

전남대학교 해양토목공학과

(2015년 11월 17일 접수, 2015년 11월 25일 수정, 2015년 12월 2일 채택)

## Investigation on the land surface temperature of industrial complexes and the non-destructive assessment of plant structures using an IR camera

Tran Quang Huy · Jung-Won Huh<sup>†</sup> · Nguyen Truong Linh · Dong-Yeob Han

*Department of Marine & Civil Engineering, Chonnam National University*

(Received 17, November 2015, Revised 25, November 2015, Accepted 2, December 2015)

### Abstract

Infrared (IR) Thermography has been recently used for a non-destructive test to acquire the necessary resources for maintenance, reparation, or replacement of structures or facilities in many industrial plants. On the other hand, it is also an effective tool in monitoring land surface temperature field for a large region via multiphase remote sensing data. In this paper, Landsat 7 ETM+ satellite images were used to calculate and compare the surface temperature of several industrial zones in Jeollanam-Do, South Korea. In addition, some of pipeline systems, tanks, and plants in a certain industrial zone were also investigated in detail by using portable infrared thermal camera, in order to measure temperature, detect steam and monitor anomalies that might exist on their facilities or structures during operation. Some common problems are also briefly discussed to provide an overview of monitoring and maintenance. Besides, a short background of IR thermal camera working principle and its initial parameters are mentioned in order to help the auditor increasing the quality of thermal images.

**Keywords :** Infrared thermography, Industrial plant, the emissivity, IR camera, remote sensing, landsat

### 1. Introduction

In many industries, they keep plants running at all times, hence predictive maintenance programs need valuable diagnostic tools for monitoring the facilities of plants such as overheated motor,

damaged insulation, high voltage power lines, pipelines and tank structures<sup>1)</sup>, IR thermal camera could be a perfect tool for this purpose. IR thermal camera can detect efficiently in two ranges of wavelength as mid-wave (2-5  $\mu\text{m}$ ) and long-wave (7.5 ~ 13.5  $\mu\text{m}$ ). However, long-wave cameras

<sup>†</sup>Corresponding author E-mail: jwonhuh@jnu.ac.kr

works well anywhere because the atmosphere tends to act as a high-pass filter above  $7.5\mu\text{m}^2$ ). Therefore, that kind of long-wavelength camera is suitable for investigating industrial plants. On the other hand, the quality of thermal images taking from IR camera is related to many factors such as the initial parameters setting in a camera, the environment, and other external effects. These issues are discussed in the following sections.

In this study, IR thermal camera was used to investigate some of pipeline systems, tanks, and plants in a certain industrial zone. For monitoring the Land Surface Temperature (LST) in a large region, Landsat 7 ETM+ data had been used to identify the temperature differences of land surface. Four industrial zones in Jeollanam-do, South Korea are inspected including Yeosu (chemical), Gwangyang (steel), Daebul (shipbuilding), and Yulchon (automobile, motorbike) in five years between 2010 and 2014. These data will help the industrial planners in developing methods of treating environmental problems.

## 2. Methodology of calculating surface temperature

The surface temperature was extracted from thermal Band 6 of Landsat 7 ETM+ images. The Landsat ETM+ sensor records temperature data and store these information as a digital number (DN) pixel values ranging between 0 and 255 in the thermal band 6.1 (wavelength from  $10.4\mu\text{m}$  ~  $12.5\mu\text{m}$ ). Then the DN is converted to spectral radiance ( $L_\lambda$ ). Radiance is then converted to brightness temperature, and

finally the brightness temperature is used to calculate surface temperature ( $T_R$ ). The following equations are used for the above progress<sup>3,4</sup>:

$$L_\lambda = \frac{L_{\max} - L_{\min}}{QCAL_{\max} - QCAL_{\min}} (DN - QCAL_{\min}) + L_{\min} \quad (1)$$

$$T_R = \frac{K_2}{\ln\left(\frac{K_1}{L_\lambda} + 1\right)} \quad (2)$$

where  $L_\lambda$  is the spectral radiance at the sensor's aperture;  $QCAL_{\max}$  and  $QCAL_{\min}$  are the highest and the lowest quantized calibrated pixel values;  $L_{\max}$  and  $L_{\min}$  are the spectral at-sensor radiance that are scaled to  $QCAL_{\max}$  and  $QCAL_{\min}$ , in  $\text{W/m}^2\cdot\text{sr}\cdot\mu\text{m}$ .

**Table 1.** Surface temperatures at four industrial zones between 2010 and 2014.

Year	Surface temperature (°C)			
	Yeosu	Gwangyang	Daebul	Yulchon
2010	17.9	18.5	12.9	10.2
2011	24.7	28.5	24.2	21.4
2012	22.4	24.5	21.0	17.8
2013	21.8	26.0	20.3	20.0
2014	25.0	28.8	24.2	21.5

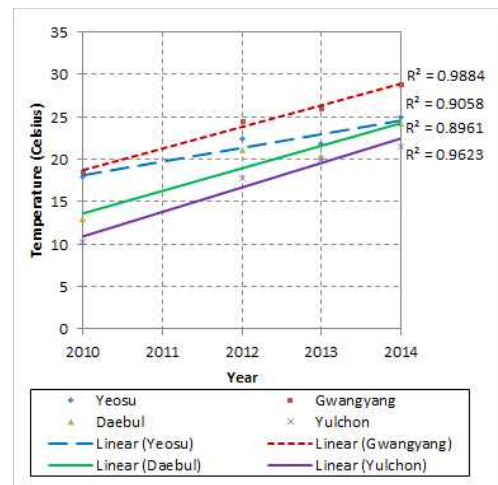


**Fig. 1.** The developing trend of temperature in four industrial zones.

The result of average surface temperatures of the studied industrial zones obtaining from satellite images, is shown in Table 1 and plotted in Fig. 1 (ignored data in 2011).

The results of surface temperature obtained from satellite images have an average difference of 0.32 °C with root mean square error of  $\pm 0.075$ , compared to Suncheon weather station<sup>5)</sup>.

It is clearly seen in Fig. 1 and in Table 1, Gwangyang has the highest average temperature among four complexes, while Yulchon has the lowest surface temperature. The reason is that Gwangyang is a steel factory, hence, it emits high temperature during the processing of steels, whereas Yulchon activities focus on machinery products, metal products, and electronic products, whose factories do not emit much heat. The second and third high temperature are Yeosu and Daebul respectively. Yeosu Industrial Complex is a petrochemical industrial park where pipeline systems and tanks are used for analyzing the products, so that surface heat emission is relatively high. Finally, Daebul is a shipyard, most of activities here are not as widespread as the other industrial zones. Therefore, the surface temperature is lower than the others<sup>5)</sup>. On the other hand, Fig. 1 (ignored data in 2011) indicates a linear correlation between time and the temperature increase. The three industrial zones Gwangyang, Daebul and Yulchon have a higher proportion of temperature growth, while the temperature at Yeosu Industrial zone increases with a more gradual slope.

Generally, surface temperature is an important parameter in monitoring the

environment, especially considering the effect of the temperature growth to nearby urban areas, for example, building protective walls, planting more trees, or even relocating local people. Together with data from satellite images, investigation of temperature pattern and other anomalies should be carried out frequently for each plant or system in every industrial zone in order to reduce the risk relative to environment and human safety. A portable IR thermal camera can be used with this purpose.

### 3. IR Camera work principle and its setting parameters

#### 3.1. Temperature measurement

The IR thermal camera measures the infrared radiation emitted from the sun and converts the detected energy into a temperature value, and then shows it on the screen or exports to image format (e.g. \*.jpg, \*.bmp). The total radiation energy received by the camera is the sum of the emission from the target object ( $W_{obj}$ ), reflected from ambient sources ( $W_{refl}$ ), and from the atmosphere ( $W_{atm}$ )<sup>6,7)</sup>, as calculated in equation (3) and illustrated in Fig. 2.

$$W_{tot} = \epsilon\sigma T_{obj}^4 + (1 - \epsilon)\sigma T_{refl}^4 + (1 - \tau)\sigma T_{atm}^4 \quad (3)$$

where  $\epsilon$  is the object emissivity,  $\tau$  is the atmosphere transmission,  $\sigma = 5.67 \times 10^{-8} \text{ W/m}^2\text{K}^4$  is the Stefan-Boltzmann constant,  $T_{obj}$  is the object temperature,  $T_{refl}$  is the reflected temperature, and the temperature of the atmosphere is  $T_{atm}$ . From the equation (3), the temperature of the object can be:

$$T_{obj} = \left[ \frac{W_{tot} - (1 - \epsilon)\tau\sigma T_{refl}^4 - (1 - \tau)\sigma T_{atm}^4}{\epsilon\tau\sigma} \right]^{1/4} \quad (4)$$

In order to obtain a correct target temperature of the object, the following parameters should be well-known: the emissivity of the object ( $\epsilon$ ), the atmospheric transmission ( $\tau$ ), the reflected temperature ( $T_{refl}$ ), and the atmospheric temperature ( $T_{atm}$ ). In addition, distance from the camera to the object, the relative humidity, and atmospheric temperature need to be used to calculate  $\tau$ , however it is normally close to one<sup>6)</sup>. In these parameters, the emissivity and the reflected temperature are the most important as discussed more in details in the following sections.

### 3.2. The emissivity of the object

The emissivity is the ratio of full-range radiant exitance ( $M$ ) of the body to full-range radiant exitance ( $M_b$ ) of a black body at the same temperature, then called the total emissivity ( $\epsilon$ ). The emissivity value from the definition is clearly from 0 to 1. The emissivity is not constant, it is a function of type of material, surface conditions, angle of observation, wavelength,

object temperature, and time<sup>6,7)</sup>.

For non-metal materials (paints, stones, concrete, etc.), the emissivity values are above 0.8. Metal materials (steel, aluminium foil, etc.) have low emissivities of below 0.2 especially with polished surface<sup>8)</sup>. Surface conditions, e.g. rough or polished, the effect is most pronounced for metals; the emissivity may be 0.07 for polished surface of steel sheet, while it could be about 0.96 if the surfaces are roughened, as seen in Table 2.

Angle of observation, in a research on a Leslie cube, the emissivity of nonmetallic materials are nearly constant from  $0^\circ$  to  $45^\circ$ , whereas it decreases gradually from

**Table 2.** Emissivity Coefficient for materials in the Industrial Zone<sup>7)</sup>

Items	Material	Emissivity
Concrete	Dry Concrete	0.95
	Rough Concrete	0.92 - 0.97
Brick	Common	0.81 - 0.86
	Fireclay	0.75
	Masonry	0.94
Wood	Plywood	0.83 - 0.98
Steel	Cold Rolled	0.75 - 0.85
	Polished sheet	0.07
	Rough surface	0.96
Others	Alloys	0.87 - 0.97
	Rubber	0.95
	Bright galvanized Zinc	0.23
	Paint (oil, flat gray)	0.92

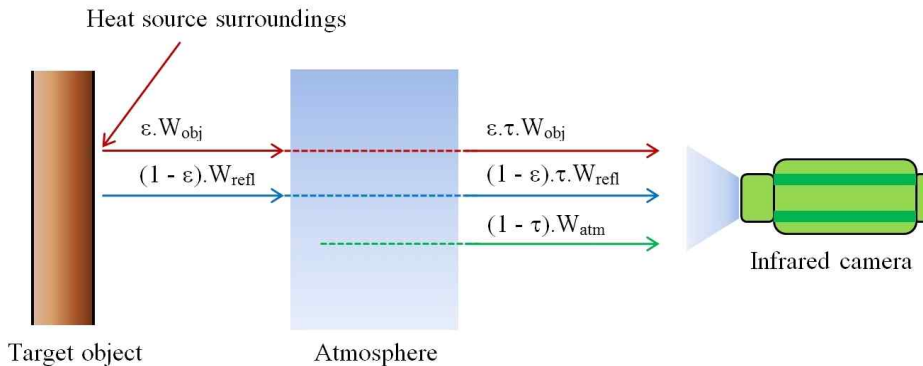


**Fig. 2.** Radiation received by an Infrared Camera.

45° to 85° . In another research on metallic materials, the behavior for larger angles found to be quite different, particularly the emissivity increasing from 45° to around 75° before decreasing<sup>8)</sup>. In a practical operation, the viewing angle should be 5° ~ 60° from perpendicular direction to avoid reflection of the IR thermal camera in the glass (e.g. for surveying building structure)<sup>4)</sup>. The emissivity values of non-metal materials increase with wavelength, whereas those for metals usually decrease<sup>8)</sup>. When the object temperature changes, the emissivity will also change due to the alteration of material properties<sup>8)</sup>.

For practical applications in thermography, the emissivity is considered as a constant and can be found in the references or guidelines of the IR camera. Several popular materials and their emissivities are listed in Table 2.

### 3.3. The Reflected Temperature

There are several methods to estimate the reflected apparent temperature. The reflector method was used for investigation in this study<sup>2,6)</sup>. The reflector method assumes the emissivity of an object as zero and a distance of zero. The steps are as follows (1) crumple up a large piece of aluminum foil; (2) attach the crinkled aluminum foil (uncrumble) on a piece of cardboard at the same size; (3) put the piece of cardboard in front of the object to be measured; (4) adjust the emissivity of the camera to 1.0, distance to zero; (5) measure the apparent temperature of the aluminum foil and write it down; and finally (6) input the temperature of the foil into the reflected temperature ( $T_{refl}$ ) setting for your infrared camera; and input the correct distance from camera to the object.

**Table 3.** Affecting factors of environment<sup>4,7,9,10,11)</sup>

Factors	Description/reasons	Recommended
Solar radiation	Change in solar irradiance over time	Solar irradiance is required 700W/m <sup>2</sup> (at least 500W/m <sup>2</sup> )
Cloud cover	Clouds will reflect infrared radiation, thereby slowing the heat transfer process to the sky.	Night-time testing should be performed during times of little or no cloud cover in order to allow the most efficient transfer of energy out of the concrete.
Temperature difference	Low temperature difference leads to bad result of thermal image	Temperature difference of at least 10 °C is advisable
Wind speed	High gust of wind might reduce surface temperatures.	For qualitative measurements, image should be taken at wind speeds of less than 25km/h <sup>12)</sup> . In fact, wind exceed 18 km/h (5 m/s) can be cautious when analyzing the data <sup>10)</sup> .
Surface moisture	Moisture tends to disperse the surface heat	Test should not be performed while the structure surface is covered with standing water
Partial shadowing (e.g. trees)	Lead to partial area of the surface cooler than other areas	Should be considered while analyzing thermal images.
Reflection	e.g. from adjacent buildings, sun, clouds.	Should be considered while surveying and analyzing thermal images.

### 3.4. Distance, relative humidity, and Atmospheric Temperature

The surveyed distance, relative humidity, and atmospheric temperature are also more three necessary parameters for IR camera automatically calculating the atmospheric transmission ( $\tau$ ). The FLIR camera's formula is as follows<sup>6,9)</sup>:

$$\tau(d, T_{atm}, \omega) = K_{atm} \cdot \exp[-\sqrt{d}(\alpha_1 + \beta_1 \sqrt{\omega})] + (1 - K_{atm}) \cdot \exp[-\sqrt{d}(\alpha_2 + \beta_2 \sqrt{\omega})] \quad (5)$$

$$\omega(\omega\%, T_{atm}) = \omega\% \cdot \exp(h_1 + h_2 T_{atm} + h_3 T_{atm}^2 + h_4 T_{atm}^3) \quad (6)$$

where  $\omega$  is the coefficient indicating the content of water vapour in the atmosphere;  $\omega\%$  is the relative humidity;  $T_{atm}$  is the atmospheric temperature in celsius degree. In this study, the CEM DT-615 equipment was used to measure  $\omega\%$  and  $T_{atm}$ .

Other parameters including distance ( $d$ ) in meter, scaling factor for the atmosphere damping ( $K_{atm} = 1.9$ ), attenuation for atmosphere without water vapour  $\alpha_1$ ,  $\alpha_2$ , and attenuation for water vapour  $\beta_1$ ,  $\beta_2$ ,  $h_1=1.5587$ ,  $h_2=6.939 \times 10^{-2}$ ,  $h_3=-2.7816 \times 10^{-4}$ , and  $h_4=6.84455 \times 10^{-7}$ . The survey distance is just around from 20m to 50m, hence the atmospheric transmission closes to one. The emission from the atmosphere ( $W_{atm}$ ) has little affected to the object temperature value.

### 3.5. Influencing factors during surveying

The temperatures measured are influenced by factors such as subsurface configurations (air void, delamination inside

the object) and initial setting parameters as mentioned above. Besides, the environment also partially plays a role in the image quality, such as cloud, wind, surface moisture, nearby obstacles, etc., see Table 3 for details and recommendations.

## 4. Applications in Investigation plant's facilities and structures

In this study, a long-wavelength infrared thermal camera FLIR SC660 was used for recording thermograms with resolution of  $640 \times 480$  pixels, thermal sensitivity  $<30$  mK at  $30^\circ\text{C}$ , Focal Plane Array (FPA) is uncooled microbolometer, and temperature is ranging from  $-40^\circ\text{C}$  to  $1500^\circ\text{C}$  with accuracy  $\pm 2^\circ\text{C}$ . The investigation was carried out on pipeline systems, tanks, and plants in an industrial zone.

### 4.1. Pipeline systems

Defects that can be detected with thermal images in pipeline systems are leakage in pumps, pipes and valves; insulation breakdowns, and pipe blockage<sup>1)</sup>.

Blocked or leakage positions could be easily located by quickly scanning the entire system before inspecting a certain position in detail. As seen in Fig. 3, some pipes were working under high temperature. Although all pipes of the system contained the same temperature liquid, some of them showed higher temperature than others. The reason can be any of the followings or their combinations; (1) pipes might be constructed with different materials, (2) pipes might have different insulation damages, (3) pipes might have different thickness due to various

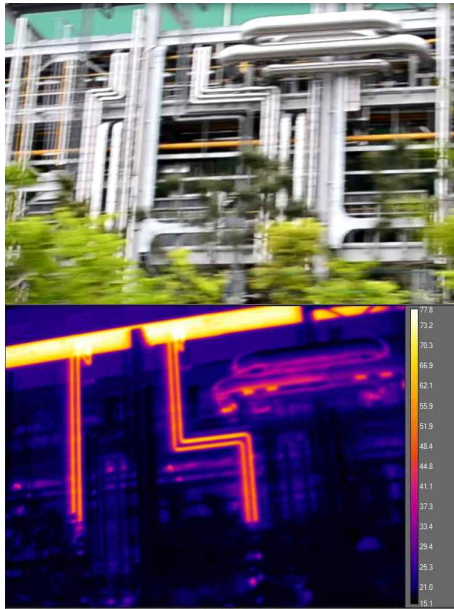


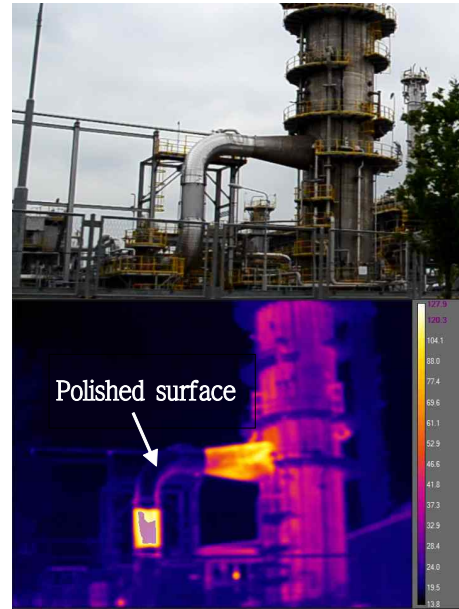
Fig. 3. Pipeline System.

environmental factors, etc.

In order to investigate if damage has occurred in the pipe system, a field test was carried out when the main system started its operation. Areas with thinner pipe are expected to respond with a faster temperature change. Alternatively, if the inspection needed to be conducted on pipes with no fluid flow, external heat sources (e.g. heat gun) can be used<sup>11)</sup>.

For a plant that consists of many different types of materials, it should be careful to set adequate emissivity for each material type. For example in Fig. 4, there is a polished surface material at the pipe elbow that shows temperature just around 20 °C to 30 °C while other parts are over 70 °C. This is because the wrong emissivity was used for the polished material.

#### 4.2. Detection of tank-level and tank cover



Thermal imaging technology can also be used for detection of tank-level, as clearly seen in Fig. 5. Besides, joints between steel curve plates of the right-hand side tank in Fig. 5 show higher temperature, indicating thicker than other areas. It may indicate that these joints are abnormal. If the thermal imaging technique can be implemented in maintenance program, it would help for early identification of damaged steel plates of the tanks. Consequently, a suitable repair or replacement can be made with a minimum cost.

When analyzing data, it is necessary to compare digital images with thermal images to avoid errors. For example the thermal image in Fig. 5, there is a low temperature rectangular area (darker color), we might think this is a deterioration, but when considering the digital image, the low temperature is due to the reflection of sunlight, as see the “reflected area” in the above digital image.

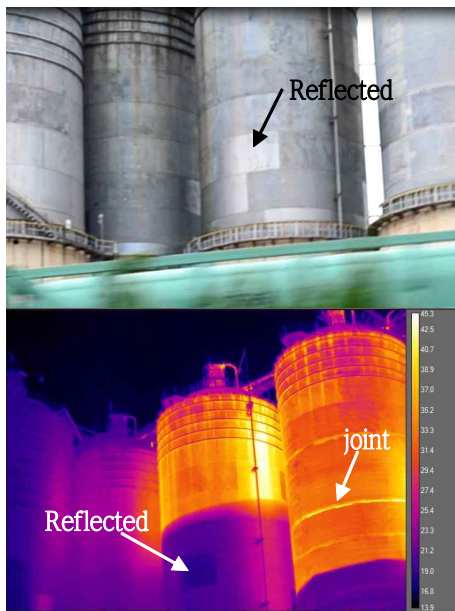


Fig. 5. Tank detection.

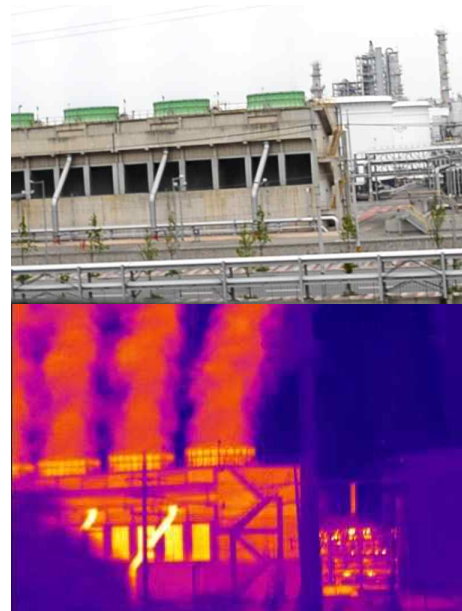


Fig. 6. Steam detection.

#### 4.3. Flare or steam detection

In order to reduce environmental impacts, harmful gases emitting from production processes gases will be burn off in flares. Unfortunately, the flames generated can be invisible to the human eye. If the flare is not burning, harmful gases might enter the atmosphere<sup>1)</sup>. In another case, as can see in Fig. 6, it is difficult to see the steam emitting from the plants by naked eyes. However, thermal imaging can easily see how much steam released to the environment. On the other hand, the plant managers can also use this application in investigating the working capacity of machineries inside the plant. For example in Fig. 6, if a chimney releases less steam than the others, we might judge that it has an anomaly in the system.

### 5. Conclusion

Infrared Thermography plays an important role in monitoring industrial plants and other large-scale structures. For measuring land surface temperature in a large area or region, thermal images can be directly derived from remotely sensed data, whereas for detail investigation, a portable infrared thermal camera is suitable to focus on every plant and its structures. The survey should be as close as possible to the surveyed object to find detail anomalies. On the other hand, the quality of thermal image not only relates to the camera quality and its resolution, having a good infrared thermography background, understanding facilities and structures of the plant, and mastering the infrared camera are also important. All of these things are human factors. In addition, the environment and other influenced factors such as nearby plants, trees, sunlight direction, wind, cloud etc. should also be taken into account when carrying out the investigation.



## Acknowledgements

The financial support from Jeonnam Green Environment Center (JNGEC, Korea) is gratefully acknowledged.

## References

1. FLIR (2011), "Thermal Imaging Guidebook for Industrial Applications", FLIR Systems Inc.
2. FLIR (2012), "The Ultimate Infrared Handbook for R&D Professionals", FLIR Systems Inc.
3. Weng Q., Lu D., Schubring J. (2004), "Estimation of land surface temperature vegetation abundance relationship for urban heat island studies", *Remote Sensing of Environment*, 89 (4), pp. 467-483.
4. FLIR (2011), "Thermal Imaging Guidebook for Building and Renewable Energy Applications", FLIR Systems Inc.
5. Linh N.T., Huy T.Q., Huh J., Han D.Y., "Land surface temperatures of industrial complexes in Jeonnam using Landsat 7 ETM+ satellite images", *Journal of the KRSA*, vol 31, No. 3, 2015, pp. 97-110.
6. Ruben Usamentiaga, et. al. (2014), "Infrared Thermography for Temperature Measurement and Non-Destructive Testing", *Sensor Journal*, 14, 12305- 12348.
7. G.C. Holst (2000), "Common Sense Approach to Thermal Imaging", SPIE Optical Engineering Press.
8. M. Vollmer, K.-P. Mollmann (2010), *Infrared Thermal Imaging - Fundamentals, Research and Applications*, Wiley-VCH, Germany.
9. IAEA (2002), "Guidebook on Non-destructive testing of concrete structures", IAEA in Austria.
10. B. Wiecek and M. Poksinska (2006), "Passive and Active Thermography Application for Architectural Monuments".
11. C.A. Balaras, A.A. Argiriou (2002), "Infrared thermography for building diagnostics", *Energy and Buildings* 34, 171-183.
12. Minkina Waldemar and Klecha Daniel (2015), "Modeling of Atmospheric Transmission Coefficient in Infrared for Thermovision Measurements", *AMA Conferences 2015 - Sensor and IRS2*.
13. FLIR (2001), "Toolkit IC2 Dig16 - Developer Guide 1.01", FLIR Systems Inc.
14. D.S. Prakash Rao (2008), "Infrared thermography and Its Applications in Civil Engineering", *The Indian Concrete Journal*.